Eur. Phys. J. A **31**, 610–612 (2007)
DOI 10.1140/epja/i2006-10208-4

THE EUROPEAN PHYSICAL JOURNAL A

Special Article – QNP 2006

Measurement of the generalized polarizabilities of the proton in virtual Compton scattering at MAMI

P. Janssens[a,b,c]

Department of Subatomic and Radiation Physics, Ghent University, 9000 Ghent, Belgium

Received: 25 October 2006
Published online: 26 February 2007 –

Abstract. Virtual Compton scattering off the proton has been studied at $Q^2 = 0.33\ (\mathrm{GeV}/c)^2$ at the MAMI accelerator in Mainz (Germany). The goal of the experiment is to measure the generalized polarizabilities (GPs) of the proton using the double polarized $\vec{e}p \to e'\vec{p}'\gamma$ reaction. This paper reports the measurement of the unpolarized photon electroproduction cross-section for the new data and the extraction of two linear combinations of GPs, which are essential for the analysis of the double spin asymmetry.

PACS. 13.60.Fz Elastic and Compton scattering – 14.20.Dh Protons and neutrons

1 Introduction

Virtual Compton scattering (VCS) off the proton ($\gamma^* + p \to \gamma + p$, where γ^* is the incoming virtual photon and γ is the outgoing real photon) is an interesting reaction to study the internal structure of the proton. Below the pion production threshold, a double polarized VCS experiment allows to measure the six lowest-order generalized polarizabilities (GPs). Two of them are an extension of the static polarizabilities, α_{E} and β_{M}, measured in real Compton scattering (RCS). α_{E} and β_{M} quantify the deformation of the charge and current distributions inside the proton caused by an external electric or magnetic field, respectively. The GPs, which are functions of Q^2, measure the polarizability locally inside the nucleon on a distance scale given by Q^2 [1]. In the real-photon limit ($Q^2 \to 0$) two of the GPs are proportional to α_{E} and β_{M}.

VCS (see fig. 1) is accessed through photon electroproduction ($ep \to e'p'\gamma$). The five-fold differential cross-section[1], $\mathrm{d}^5\sigma/\mathrm{d}k'\mathrm{d}\Omega_{e'}\mathrm{d}\Omega_{p',\mathrm{cm}}$, depends on the virtual photon momentum q_{cm} and its polarization parameter ε, the real (outgoing) photon momentum q'_{cm} and the polar and azimuthal angle of the real photon with respect to the virtual photon direction, $\theta_{\gamma\gamma,\mathrm{cm}}$ and φ.

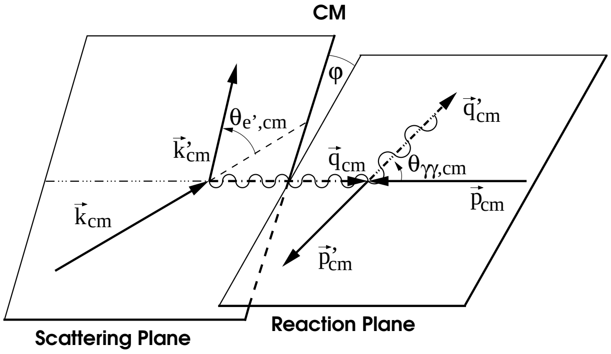

Fig. 1. Schematic drawing of the $ep \to e'p'\gamma$ reaction in the center of mass of the virtual photon and the target proton.

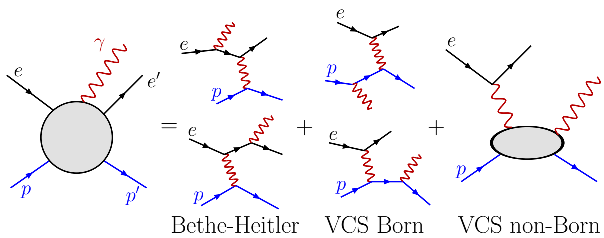

Fig. 2. Decomposition of the $ep \to e'p'\gamma$ reaction.

The photon electroproduction reaction contains three contributions (see fig. 2): the reaction is dominated by the Bethe-Heitler and Born (BH+B) contributions, where the outgoing photon is produced due to Bremsstrahlung of the electron or proton, respectively. The contribution of the BH+B process can be calculated exactly based on the proton form factors. The GPs contribute to the VCS non-Born part of the reaction.

---

[a] e-mail: peter@inwfsun1.ugent.be

[b] On behalf of the VCS Collaboration at MAMI-A1.

[c] Aspirant of the FWO.

[1] All variables defined in the center of mass of the virtual photon and target proton have an index "cm". If no index is given the variable is defined in the laboratory system.

2 Experimental determination of the GPs

The GPs cannot be measured directly. In the physical observables (cross-sections and asymmetries) they appear in specific linear combinations, the structure functions. Since there are six independent GPs, there are six independent structure functions [2].

2.1 Unpolarized cross-section

The low-energy theorem (LET) can be used to expand the unpolarized cross-section in powers of $q'_{\rm cm}$ ([1] and [2]):

$$\mathrm{d}^5\sigma = \mathrm{d}^5\sigma^{\rm BH+B} + \phi q'_{\rm cm}\Psi_0 + \mathcal{O}\left({q'_{\rm cm}}^2\right), \quad (1)$$

where ϕ is a known phase space factor, $\mathrm{d}^5\sigma^{\rm BH+B}$ is the five-fold differential cross-section for the BH+B processes and Ψ_0, which contains the information about the GPs, is defined by

$$\frac{\Psi_0}{v_{\rm LT}} = \frac{v_{\rm LL}}{v_{\rm LT}}(P_{\rm LL} - P_{\rm TT}/\varepsilon) + P_{\rm LT}\,. \quad (2)$$

In this equation $v_{\rm LT}$ and $v_{\rm LL}$ are kinematical coefficients (containing, *e.g.*, $\theta_{\gamma\gamma,\rm cm}$), and $P_{\rm LL}$, $P_{\rm TT}$ and $P_{\rm LT}$ are the structure functions one wants to measure. The higher-order terms $\mathcal{O}({q'_{\rm cm}}^2)$ can be neglected for low $q'_{\rm cm}$, a condition which holds below the pion production threshold. In eqs. (1) and (2) two linear combinations of structure functions appear ($P_{\rm LL} - P_{\rm TT}/\varepsilon$ and $P_{\rm LT}$), which can be separated by measuring the unpolarized cross-section in an appropriate kinematical region (see sect. 4).

2.2 Double spin asymmetry

More information about the GPs can be extracted from polarized observables. One wants to use the low-energy theorem to extract the GPs from the data, for which the experiment should be performed below the pion production threshold. Since in that regime all single spin asymmetries for VCS disappear [2], one has to perform a double polarized experiment (here $\boldsymbol{e}p \to e'\boldsymbol{p}'\gamma$). The double spin asymmetry (DSA) along the axis i in the center of mass is defined by

$$P_i = \frac{\mathrm{d}^5\sigma_i^{\uparrow} - \mathrm{d}^5\sigma_i^{\downarrow}}{\mathrm{d}^5\sigma_i^{\uparrow} + \mathrm{d}^5\sigma_i^{\downarrow}} = \frac{\Delta\mathrm{d}^5\sigma_i}{2\mathrm{d}^5\sigma} \qquad (i = x, y, z)\,. \quad (3)$$

$\mathrm{d}^5\sigma_i^{\uparrow}$ represents the differential cross-section, where the outgoing proton is polarized along the i-axis and the helicity, h, of the incoming electron equals $+\frac{1}{2}$, indicated by $\uparrow$ ($\downarrow$ corresponds to $h = -\frac{1}{2}$). The axes of the reference frame in the center of mass are defined as in [2].

The denominator is two times the unpolarized cross-section (see sect. 2.1). Similarily to the unpolarized cross-section, the low-energy theorem can be used to write the numerator as

$$\Delta\mathrm{d}^5\sigma_i = \Delta\mathrm{d}^5\sigma_i^{\rm BH+B} + \phi q'_{\rm cm}\Delta\Psi_{0,i} + \mathcal{O}\left({q'_{\rm cm}}^2\right), \quad (4)$$

where the terms $\Delta\Psi_{0,i}$ ($i = x, y, z$) are linear combinations of the structure functions:

$$\Delta\Psi_{0,z} = v_1^z P_{\rm TT} + v_2^z P_{\rm LT}^z + v_3^z P_{\rm LT}^{\prime z}\,, \quad (5)$$

and similar expressions for $\Delta\Psi_{0,x}$ and $\Delta\Psi_{0,y}$ (see [2]). In these three terms $\Delta\Psi_{0,i}$ the six independent structure functions appear, thus one can determine all six GPs by measuring the DSA for VCS.

3 Experimental setup

For the present experiment the standard setup of the A1 hall at MAMI was used [3]: the longitudinally polarized electron beam from the MAMI accelerator impinges with an energy of 854.6 MeV on a liquid-hydrogen target. The polarization of the beam is about 75%. The scattered electron and recoiling proton are detected in the high resolution magnetic spectrometers.

Real photon production events are identified by missing-mass reconstruction. The central momenta and angles of the spectrometers were optimized to detect real-photon production events with $q_{\rm cm} = 600\,\mathrm{MeV}/c$, $q'_{\rm cm} = 90\,\mathrm{MeV}/c$, $\varepsilon = 0.645$ and $\varphi = 0°$.

To measure the polarization of the recoiling proton a polarimeter was mounted behind the tracking detectors of spectrometer A. It consists of a 7 cm carbon scattering block and two double planes of horizontal drift chambers ([4] and [5]) and it allows to measure the transverse components of the proton polarization in the focal plane.

The magnetic field of the spectrometer rotates the spin of the protons on their way to the focal plane. This precession mixes the different components of the proton polarization, dependent on the magnetic field along the proton track in the spectrometer. This allows to measure the three components of the proton polarization in the center-of-mass system.

4 Preliminary results

The first step in the analysis of the experiment is the determination of the absolute unpolarized cross-section of the $ep \to e'p'\gamma$ reaction. Since the effect of the GPs is about 10% on the total cross-section, the solid angle of the detector acceptance has to be calculated accurately. This is performed using a Monte Carlo simulation [6], which incorporates all relevant resolution deteriorating effects. The events in the simulation are generated according to the BH+B cross-section behaviour, which is a very good approximation of the real cross-section for the kinematics of the experiment.

The measured cross-section is shown in fig. 3. The dotted line shows the BH+B contribution; the full line shows a fit to the data points and includes the effect of the GPs. This fit is shown in fig. 4, where $\Psi_0/v_{\rm LT}$ is plotted *versus* $v_{\rm LL}/v_{\rm LT}$ (see eq. (2)). The results of the fit are shown in table 1. The first error indicates the statistical error.

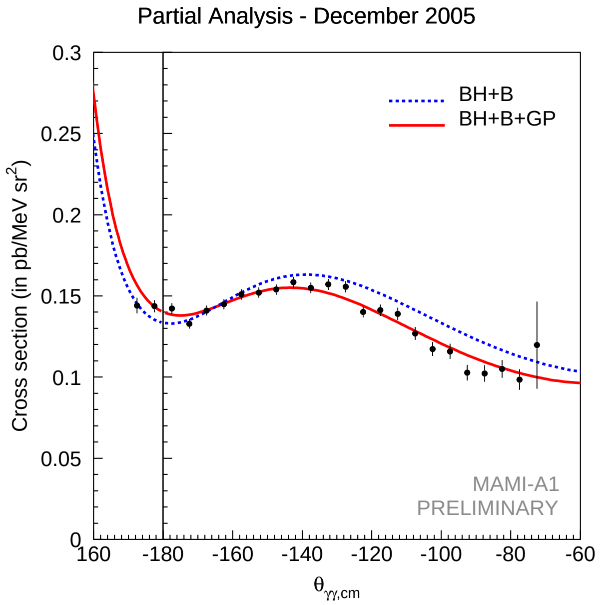

Fig. 3. The unpolarized $ep \to e'p'\gamma$ cross-section $\mathrm{d}^5\sigma/\mathrm{d}k'\mathrm{d}\Omega_{e'}\mathrm{d}\Omega_{p',\mathrm{cm}}$ measured at $q'_{\mathrm{cm}} = 90$ MeV$/c$, $q_{\mathrm{cm}} = 600$ MeV$/c$, $\varepsilon = 0.645$ and $\varphi = 0°$. The dotted line shows the BH+B cross-section, which deviates from the measured five-fold differential cross-section due to the contribution of the GPs. The full line shows the result of the fit in fig. 4. Negative values of $\theta_{\gamma\gamma,\mathrm{cm}}$ correspond to $\varphi = 180°$.

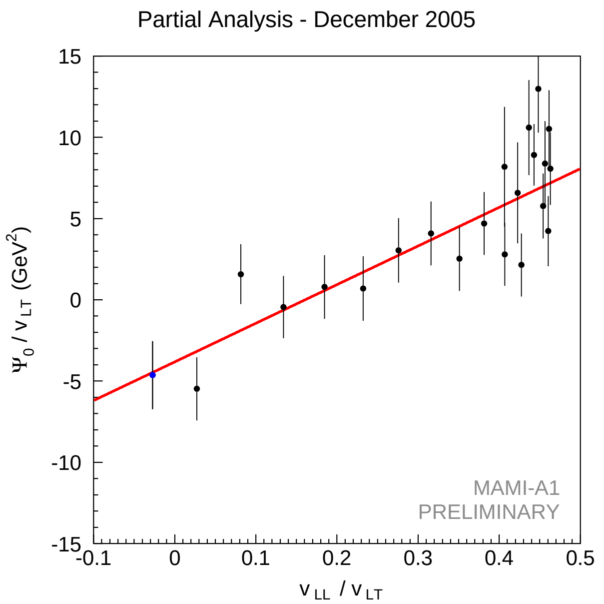

Fig. 4. A linear fit of Ψ_0/v_{LT} *versus* $v_{\mathrm{LL}}/v_{\mathrm{LT}}$ yields two linear combinations of GPs: $P_{\mathrm{LL}} - P_{\mathrm{TT}}/\varepsilon$ and P_{LT} (see eq. (2)). The reduced χ^2 of the fit is 1.35.

Table 1. Results for $P_{\mathrm{LL}} - P_{\mathrm{TT}}/\varepsilon$ and P_{LT} for $q_{\mathrm{cm}} = 600$ MeV$/c$. The meaning of the different errors is explained in the text. ε in reference [7] ($\varepsilon = 0.620$) was slightly different from the present experiment ($\varepsilon = 0.645$).

	$P_{\mathrm{LL}} - P_{\mathrm{TT}}/\varepsilon$ (GeV^{-2})	P_{LT} (GeV^{-2})
This work	$23.8 \pm 2.9 \pm 0.3 \pm 3.5$	$-3.8 \pm 1.0 \pm 0.9 \pm 1.1$
Ref. [7]	$23.7 \pm 2.2 \pm 0.6 \pm 4.3$	$-5.0 \pm 0.8 \pm 1.1 \pm 1.4$

The two other errors are the contributions of the absolute normalization of the cross-section and the absolute calibration of the spectrometers' central momentum to the systematic error, respectively. The result is in good agreement with the previous experiment [7].

In the next step the DSA will be determined. The DSA is defined in the center of mass (see sect. 2.2). Similar to the analysis of polarized pion electroproduction the Wigner rotation of the proton spin due to the Lorentz boost from the center of mass to the laboratory system has to be taken into account [8].

The GPs will be fitted to the data via the DSA along the x-, y- and z-axis using a maximum-likelihood method. The values for $P_{\mathrm{LL}} - P_{\mathrm{TT}}/\varepsilon$ and P_{LT} obtained in the unpolarized analysis are used as a constraint for this fit. This analysis is in progress.

This work was supported in part by the FWO-Flanders (Belgium), the French CEA and CNRS/IN2P3, the Deutsche Forschungsgemeinschaft (SFB 201 and SFB 443) and by the Federal State of Rhineland-Palatinate.

References

1. P.A.M. Guichon *et al.*, Nucl. Phys. A **591**, 606 (1995).
2. P.A.M. Guichon *et al.*, Prog. Part. Nucl. Phys. **41**, 125 (1998).
3. K.I. Blomqvist *et al.*, Nucl. Instrum. Methods A **403**, 263 (1998).
4. Th. Pospischil *et al.*, Nucl. Instrum. Methods A **483**, 713 (2002).
5. Th. Pospischil *et al.*, Nucl. Instrum. Methods A **483**, 726 (2002).
6. P. Janssens *et al.*, Nucl. Instrum. Methods A **566**, 675 (2006).
7. J. Roche *et al.*, Phys. Rev. Lett. **85**, 708 (2000).
8. H. Schmieden *et al.*, Eur. Phys. J. A **1**, 427 (1998).